

Modeling and optimization of SOFC based on Metaheuristics

Qixiang Wu^{1,*}, Mohammadreza Shafiee²

¹ Media Design Department, Woosong University, Daejeon, Republic of Korea

² Semnan University, Semnan, Iran

*E-mail: shiping1737@163.com, shafiee21@gmail.com

Received: 9 April 2020 / Accepted: 13 August 2020 / Published: 30 September 2020

This study proposed a well-organized technique for the optimal selection of the unknown parameters for the Solid Oxide Fuel Cell (SOFC) model. The main idea is to propose a new metaheuristic method to achieve more efficient results for the model to give a satisfying agreement between the voltage and current profile of the SOFC. The mean squared error (MSE) has been adopted as an objective function between the achieved data and the experimental data. For minimizing the MSE, a new modified version of the Stain Bowerbirds Optimization algorithm has been utilized. The proposed design is applied to simulated data and practical data to verify its efficiency. Finally, the robustness and the precision of the presented algorithm are compared and verified by some state of art metaheuristics including basic Satin Bowerbird Optimization algorithm (SBO), Differential evolution algorithms (DE), coRNA-GA, Chaotic Binary Shark Smell Optimization (BSSO), and Swarm Optimizer (SO).

Keywords: Solid Oxide Fuel Cell; model estimation; Stain Bowerbirds Optimization algorithm; electrochemical model.

1. INTRODUCTION

However, fossil fuels are now the main part of energy resources in the world, due to some main disadvantages like generating a high ratio of pollutants and also the lack of fossil fuel resources leads the researchers to work a clean alternative energy resource [1,2]. Fuel cells are a kind of clean energy resources that their applications have been increasing [3]. Fuel cell technology has been the focus of research in recent years due to its high efficiency, lower pollution, use of different fuels, and flexibility in the type of energy produced [4-6]. Other benefits of a fuel cell include adaptability to the environment, lack of noise pollution due to the lack of moving parts, the ability to generate heat and electricity at the same time, and use in decentralized energy production applications [7,8]. Among the different types of fuel cells, only those cells can be used in power plants that have high operating temperatures. Therefore, Solid Oxide Fuel Cell (SOFC) is the main option for employing power plants [9,10]. Because in addition

to the overall benefits of fuel cells, the specific benefits of SOFCs, including higher efficiency than other fuel cells, the possibility of using the heat generated in the fuel cell (stack) for increased efficiency, the possibility of reforming the inlet fuel inside the fuel cell stack due to its high operating temperature, not needing for expensive catalysts and the low corrosion problem due to the use of solid electrolyte in its structure has increased the use of this type of fuel compared with other kinds of fuel cells [11]. As mentioned above, the exhaust gases from the solid oxide fuel cell have a high temperature so that the heat of these gases can be used to increase re-efficiency [12,13]. For example, the SOFC gas power plant can be studied as an upstream cycle for either single or multi-pressure CHP Rankine cycles [9]. Generally, the mathematical modeling of SOFCs gives basic information of them that is significant for optimal designing of the system by considering physical and electrochemical reactions [14]. This case encourages the researchers to work on better modeling of this kind of fuel cell. Several methods have been proposed in this field. For example, Yang [15] proposed an optimized procedure for the optimal selection of the dynamic model of SOFC. A three sub-models were used for the SOFC. Improved Genetic Algorithm (IGA) was used for the parameter optimization. The proposed improved algorithm was validated by some different types of GA in terms of accuracy.

Liu [16] presented an adaptive technique based on the Differential Evolution (DE) algorithm for the optimal selection of the model parameters. For achieving better results of the method, the crossover technique has been added to the algorithm. For validating the proposed method, it is applied to a simple electrochemical SOFC model. The simulation showed that the presented method has better efficiency for the identification of model parameters compared with other metaheuristics from the literature.

Wei [17] proposed an optimization method for optimal modeling of the SOFC system. The main idea is to achieve optimum value parameters for the solid oxide fuel cell by minimizing the mean squared deviation error based on a modified version of Binary Shark Smell Optimizer and Chaos theory. MATLAB software was used for simulating the method. The method was applied to empirical data and the results also compared with some other state of art techniques to indicate the method capability.

Jun [18] introduced an optimized procedure to minimize the system cost once an air leakage fault occurs and to maximize the total performance of the SOFC. These two objectives lead the researchers to use a non-dominated sorting PSO algorithm. The simulation results indicated that the presented method gave a maximum performance and minimum cost for the studied SOFC.

Bunin [19] performed an empirical verification of a real-time optimization (RTO) for the efficient operation of SOFCs. The RTO adopted the constraint-adaptation methodology to supply the constraints. The impact of the filter parameters was implemented to a modifier update and of the RTO frequency for more investigation. Based on the literature it can be concluded that several studies have been presented for parameter identification of a SOFC in both transient and steady-state scenarios. The purpose of the present research is to design a new reliable approach for parameter estimation of SOFC. The main contribution of the present work is briefly given below:

- A new optimal method based on metaheuristics is proposed for SOFC model identification
- The MSE is used as a cost function between the achieved and the experimental data
- A modified version of Stain Bowerbirds Optimization algorithm is utilized for minimizing MSE
- The method is verified by simulated data and practical data
- The robustness and the precision of the method are compared with some state of art methods

2. THE DYNAMIC MODEL OF SOLID OXIDE FUEL CELL

As previously mentioned, for achieving a proper optimized SOFC model, we need to represent and simulate it before the construction. In this study, a dynamic model of SOFC is proposed for optimal parameter identification. The dynamic electrochemical model of the SOFC has been described in the following. Based on [16,9,20,13], the output voltage of a single SOFC is obtained as follows:

$$V_{cell} = E_{Nernst} - V_{\Omega} - V_{conc} - V_{act,cell} \quad (1)$$

where, E_{Nernst} describes the Nernst voltage, V_{Ω} stands for the ohmic loss, V_{conc} represents the concentration loss, and V_{act} defines the activation loss. By considering the above definition, the output voltage for the SOFC stack including N_{cell} number of cells is as follows:

$$V_{stack} = N_{cell} \times V_{cell} = E_{Nerst} - E_{\Omega} - E_{conc} - V_{act} \quad (2)$$

In Eq. (2), the Nernst reversible voltage is achieved as follows [20]:

$$E_{Nerst} = E_0 + \frac{R \times T}{4 \times F} \ln \left(\frac{P_{H_2}^2 \times P_{O_2}}{P_{H_2O}^2} \right) \quad (3)$$

where, E_0 describes the standard potential, T stands for the operating temperature of the SOFC (K), P_{H_2} , P_{O_2} , and P_{H_2O} describe the partial pressure of hydrogen oxygen, and water. $R = 8.314 \text{ kJ} (kmol \text{ K})^{-1}$ determines the universal gas constant, $F = 96,486 \text{ C mol}^{-1}$ describes the Faraday constant.

By considering Eq. (2), the ohmic resistance happens once the resistance of ions to the flow in the electrolyte and their resistance to the electrons flow over the electrode materials. The general ohmic voltage loss is achieved as follows:

$$V_{\Omega} = I \times R_{\Omega} \quad (4)$$

where, R_{Ω} describes the ionic resistance, which is gradually reduced by increasing temperature[9]. Based on the ButlerVolmer equation, the loss of activation voltage is achieved as follows [21]:

$$I = I_0 \times \left\{ \exp \left(\frac{\beta \times n_e \times F \times V_{act,cell}}{R \times T} \right) - \exp \left(\frac{(\beta - 1) \times n_e \times F \times V_{act,cell}}{R \times T} \right) \right\} \quad (5)$$

where, β represents the transfer coefficient, I_0 describes the density for the exchange current, n_e defines the transferred electrons mole quantity. By considering [16], $\beta = 0.5$ and therefore:

$$I = 2 \times I_0 \times \sinh \left(\frac{n_e \times F \times V_{act,cell}}{2 \times R \times T} \right) \quad (6)$$

Accordingly,

$$V_{act,cell} = \frac{2 \times R \times T}{n_e \times F} \times \sinh^{-1} \left(\frac{I}{2 \times I_0} \right) \quad (7)$$

The concentration voltage loss happens once the resistance of mass transfer to the reactants and products flow over the porous electrodes. Since the concentration voltage loss is obtained by the following equation:

$$V_{conc} = \frac{R \times T}{4 \times F} \times \left[\ln \left(\frac{P_{H_2}^2 \times P_{O_2}}{P_{H_2O}^2} \right) - \ln \left(\frac{P_{H_2}^{*2} \times P_{O_2}^*}{P_{H_2O}^{*2}} \right) \right] \quad (8)$$

The present study presents a simple electrochemical model for the SOFC stack as for the output efficiency. Based on [22], the SOFC output voltage can be simplified as follows:

$$V_{stack} = E_0 - A \times \ln\left(\frac{I}{I_0}\right) - I \times R_\Omega + B \times \ln\left(\frac{I_L - I}{I_L}\right) \quad (9)$$

where, A describes the Tafel line slope, B is a constant depends on the operating state of the fuel cell, I_L represents the density of the limit current (mA cm^2). R_Ω stands for the area-specific resistance in ($\text{k}\Omega \text{ cm}^2$), and E_0 defines the open-circuit voltage.

Because of the second term of Eq. (9) is the Tafel equation, which is generally employed under a high activation polarization and because of the reason that the Tafel equation makes high errors during low activation polarization, the ButlereVolmer equation is performed to define the activation voltage loss as follows [23]:

$$V_{stack} = E_0 - A \times \sinh^{-1}\left(\frac{I}{2 \times I_0^a}\right) - A \sinh^{-1}\left(\frac{I}{2 \times I_0^c}\right) - I \times R_\Omega + B \times \ln\left(\frac{I_L - I}{I_L}\right) \quad (10)$$

where, I_0^c and I_0^a represent the density of the cathode and the anode exchange currents, respectively.

In this research, seven main parameters have been selected for optimal parameters selection including E_0 , A , B , I_0^a , I_0^c , R_Ω , and I_L , i.e. the decision vector x can be considered by the following equation:

$$x = [E_0, A, B, I_0^a, I_0^c, R_\Omega, I_L] \quad (11)$$

3. THE COST FUNCTION

For optimal parameter selection of the SOFC stack model, a cost function is needed. The presents study uses the mean squared error (MSE) as the cost function:

$$\min fit(x) = \frac{1}{n} \sum_{i=1}^n (V_{out} - V_{est})^2 \quad (12)$$

where, n stands for the number of data for estimation, and $x = \{x_1, x_2, x_3, x_4, x_5, x_6, x_7\} = \{E_0, A, B, I_0^a, I_0^c, R_\Omega, I_L\}$ are the optimization variables.

Such that [24],

$$\underline{x}_j \leq x_i \leq \bar{x}_i \quad (13)$$

$$L \leq I_L, i = 1, 2, \dots, n \quad (14)$$

$$I_0^c < I_0^a \quad (15)$$

To achieve high conformity between the actual data and the estimated model, a minimum value should be achieved for Eq. (12) that is performed by optimal selection of the undetermined parameters (x) with its constraint in Eqs. (13-15).

There are different types of optimization methods to solve such problems. The classic optimization algorithms are the first selection for the optimization which is due to their exact solutions. Recently, due to increasing the complexity of the problems, these methods not only usually fail to give a proper solution to solve the complicated problems, but also, they sometimes stuck in the local optimum. In recent years, the development of metaheuristics as simple and global optimizers turn them as the first

option to solve these optimization problems [25,26]. In recent research, a modified version of a new modified metaheuristic method, called Chaos Satin Bowerbird Optimization algorithm is used for the optimal selecting of the SOFC parameters for identification problems.

4. SATIN BOWERBIRD OPTIMIZATION ALGORITHM

Satin Bowerbird is a marvelous kind of bird that lives in Australia. Among the wonders of this bird is that has a big talent in the case of nesting such that its nest is similar to a bower. During the mating season, a male satin bowerbird attempts to build the best beautiful bower for attracting female bowerbirds. This is a competitive process among males to attract the female by designing better bower. The bower designing is performed by collecting different things such as their small twigs, ornamental stones, and other beauties.

Afterward, a female satin bowerbird comes to the bower in from the backside when the males are absent. Then, the female goes back to judge the male. Once numerous bowers are in the same general area, females can analyze males with higher speed and watch them all as their bowers take shape. These features inspired

Moosavi works on a new version of metaheuristics based on these interesting birds that are called the Satin Bowerbird Optimization algorithm (SBO) [27]. In the following, the method of designing the SBO algorithm has been explained.

4.1. Initializing

The SBO is a population-based algorithm that starts with some uniform and random n -dimensional population vector that defines the positions of the bowers. The attractiveness of each male bower is made by a combination of different parameters. Consider the initial population of the SBO as follows:

$$W_h = (w_1, w_2, \dots, w_m) \quad (16)$$

where, W_h describes the h^{th} solution and (w_1, w_2, \dots, w_m) is the population of the solution.

The attractiveness of the bowers is defined by the probability of fitness value. Therefore, probability helps the satin female bowerbirds to select the best male. Once a male bowerbird has been selected by the female based on its probability, it mimics the bower construction, i.e.

$$Prob_i = \frac{fit_i}{\sum_{n=1}^{NB} fit_n} \quad (17)$$

$$fit_i = \begin{cases} \frac{1}{1 + f(x_i)}, & f(x_i) \geq 0 \\ 1 + |f(x_i)|, & f(x_i) < 0 \end{cases} \quad (18)$$

where, $f(x_i)$ represents the value of the cost function for the position i .

4.2. Elitism

The SBO algorithm considered the best individual as *elitism*. Essentially, all the male satin bower birds make their bowers based on their instinct such that each of them uses its unique instinct for making the bower in the mating season. However, the male satin bower birds utilize unique materials for their bower decorating, they also use their experiences as the main factor for more attraction of the female satin bowerbirds. In other words, experience has a high significance on both bower construction and dramatic gestures that help elder males to have more power for attracting the females to their bower. The algorithm considers the bower with the best position as the elite of the current iteration. Elites have a high ability to effect on the other positions updating.

4.3. Updating

The updating process of the positions in each cycle of the algorithm is done by the following formula:

$$W_{hj}^{new} = W_{hj}^{old} + \lambda_j \left(\frac{W_{ij} + W_{elite,j}}{2} \right) - W_{hj}^{old} \quad (19)$$

where, W_i describes the desired solution in the current iteration, i is obtained by roulette wheel methodology, W_{hj} describes the j^{th} member of W_h , W_{elite} represents the elite's position, λ_j defines the attraction power in the desired bower (solution) that is calculated as follows:

$$\lambda_j = \frac{\alpha}{1 + p_i} \quad (20)$$

where, α describes the greatest step size of the solution and p_i defines the probability achieved by $Prob_i$.

4.4. Mutation

Due to the seriousness of the competition, the weaker male satin bower birds are may be attacked by stronger ones or even totally ignored by the others, such that stronger males may destroy the weaker males' bower or steal their materials. This behavior has been applied to the algorithm by performing a specific probability to W_{hj} ; therefore, a normal distribution (L) can be adopted with variance σ^2 and average of W_{hj}^{old} as follows:

$$w_{hj}^{new} \sim L(w_{hj}^{old}, \sigma^2) \quad (21)$$

$$L(w_{hj}^{old}, \sigma^2) = w_{hj}^{old} + (\sigma \times L(0,1)) \quad (22)$$

The proportion of space width is represented as a value of α that is evaluated in equation (16).

$$\alpha = y \times (Var_{max} - Var_{min}) \quad (23)$$

where, y stands for the variance ratio among lower and upper ranges, var_{max} and var_{min} represent the upper and the lower limits assigned by the variable.

All the populations have been then combined and sorted to generate the new population. Once the termination condition satisfied, the algorithm has been stopped.

4.5. Satin Bowerbird Optimization algorithm based on chaos theory (ISBO)

However, the SBO algorithm gives promising results for the optimization problems, its low convergence speed in some problems makes a weak solution or even an improper solution. In this study, two mechanisms are employed for decreasing this problem as it is possible. The first term is to use a Quasi-oppositional learning mechanism. For understanding the conception of this mechanism, we first define the basic oppositional learning mechanism. The oppositional learning mechanism is a method for modifying the premature convergence problem by comparing each individual of the population with its opposite value and to select the better one as a more suitable candidate [28,29]. This mechanism is performed by assuming a candidate x as a real number in the search space with d -dimension in the range $[\alpha, \beta]$. In this situation, the opposite mechanism for the individual x is obtained as follows:

$$\tilde{x}_i = \alpha_i + \beta_i - x_i \quad (24)$$

$$i = 1, 2, \dots, D \quad (25)$$

By considering the definition of the opposite mechanism, the quasi-opposite number is obtained as follows [30]:

$$\hat{x}_i = rand \left(\frac{\alpha_i + \beta_i}{2}, \tilde{x}_i \right) \quad (26)$$

The above mechanism is used for better population generation.

The second mechanism employed in this study is to use the chaotic mechanism. Based on the chaos theory, the real nature of systems is complicated and nonlinear, and also some models seem random, but they have a formulated pseudo-random nature [31,32]. This mechanism is utilized to speed up the quasi-opposite by using pseudo-random values instead of random values in each iteration. The present study uses the logistic map as a chaotic mechanism to modify the quasi-opposite mechanism. The logistic map is formulated below [31,32]:

$$\delta_{o,n}^{q+1} = 4\delta_{o,n}^q(1 - \delta_{o,n}^q) \quad (27)$$

where, o describes the value of the system generators, n stands for the number of populations, q represents the number of iterations, δ_n is the chaotic mechanism value in iteration n that is placed between 0 and 1.

Based on the above explanations, the new population in the next iteration will be generated by the following equation:

$$\hat{x}_n^{q+1} = \delta_{o,n}^q \times \hat{x}_n^q \quad (28)$$

Fig. (1) indicates the flowchart diagram of the ISBO algorithm.

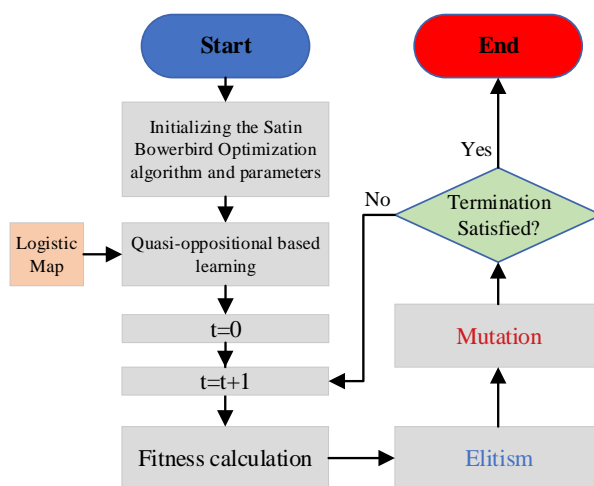


Figure 1. The flowchart of the ISBO algorithm

5. SIMULATION RESULTS

The programming has been simulation based on MATLAB 2017b software based on CPU: Intel Core i7-4720-HQ 2.60 GHz; RAM: 16 GB with Microsoft Windows 10 Enterprise Edition operating system. For applying the estimation of the parameters of the SOFC, the ISBO algorithm parameter values of the mutation probability are considered 0.05, α and z are considered 0.95 and 0.03, respectively, and the initial population and maximum iteration are selected 50 and 1000, respectively. Based on the aforementioned discussions, the efficiency of the parameter identification of the SOFC with the presented technique has been validated by implementing it to a dynamic electrochemical model from [9]. Table 1 indicates the operating conditions for the analyzed SOFC model.

Table 1. The operating conditions for the analyzed SOFC model [9]

Parameter	Value	Unit
Cell number	96	-
Load current	0-158	A
The mass flow rate of the Air	0.012	mol s ⁻¹
The mass flow rate of the H2	9E-4	mol s ⁻¹
H2O mass flow rate	1E-4	mol/s
Anode and Cathode pressure	3	atm
Inlet temperature for fuel and Air	899.85	°C

5.1. Validation based on simulated data

The simulation has been performed to different temperatures including 799.85 °C, 849.85°C, 899.85°C, 949.85°C, and 999.85°C) and different pressures including 1 atm, 3 atm, 5 atm, 7 atm, and 9 atm. The range of the limitations of the parameters has been given in Tables 2.

Table 2. The feasible range of the unknown parameters for optimization

Parameter	Range	Unit	Parameter	Range	Unit
E_{OC}	[0, 1.2]	V	B	[0,1]	V
A	[0, 1]	V	I_L	[0,10000]	$mA.cm^{-2}$
$I_{0,a}, I_{0,c}$	[0,100]	$mA.cm^{-2}$	R_{ohm}	[0,1]	$K\Omega.cm^{-2}$

For the simulation, the data sets have about 16,000 data points such that only about 1600 numbers have been adopted from the main dataset with a step size of 10 to speed up the process. The feasible range of the unknown parameters is considered based on Table 2. Table 3 and Table 4 illustrate the estimated parameters for the simulated data by different temperatures and pressures based on the proposed improved SBO algorithm. For determining the value of the error, the MSE values are also given in Tables. Figs. (2) and (3) show the comparisons of the results for the voltage-current profile of the simulated data and the estimated data based on the improved SBO algorithm at different pressures and temperatures.

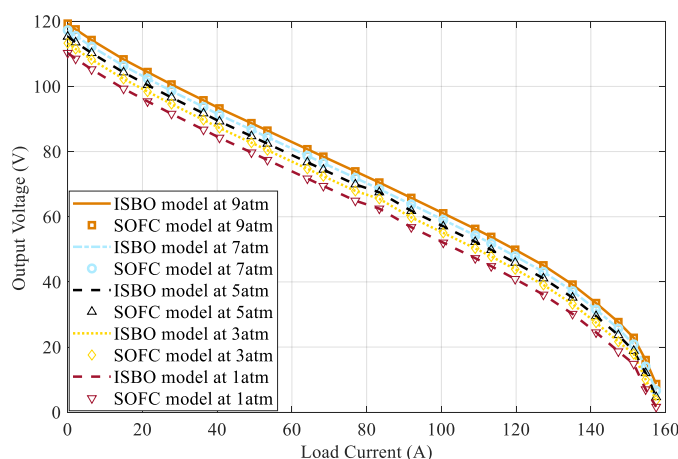


Figure 2. The comparisons of the results for the voltage-current profile of the simulated data and the estimated data based on the ISBO algorithm at various pressures

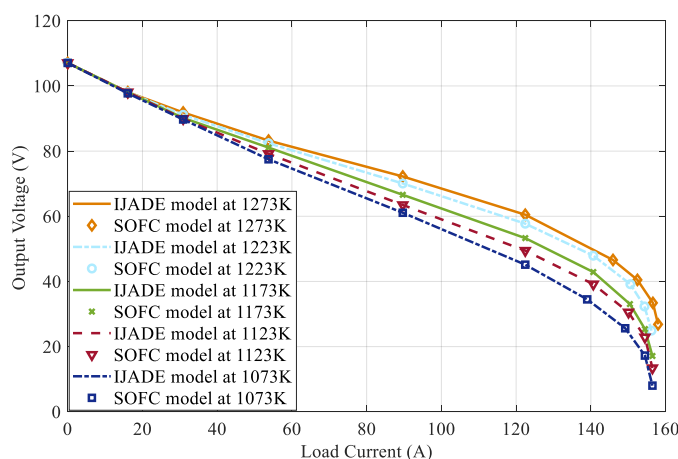


Figure 3. The comparisons of the results for the voltage-current profile of the simulated data and the estimated data based on the ISBO algorithm at various temperatures

Table 3. The estimated parameters for the simulated data by various temperatures based on the ISBO algorithm

Variables	799.85 °C	849.85°C	899.85°C	949.85°C	999.85°C
$E_{oc}(V)$	1.127	1.123	1.115	1.110	1.108
$A(V)$	0.041	0.037	0.033	0.029	0.025
$I_{o,a}(mA.cm^{-2})$	32.834	28.336	25.634	23.059	20.637
$I_{o,c}(mA.cm^{-2})$	6.830	5.751	4.397	3.695	3.108
$B(V)$	0.068	0.072	0.076	0.078	0.083
$I_L(mA.cm^{-2})$	158.93	159.67	160.27	160.29	160.31
$R_{ohm}(K\Omega.cm^{-2})$	0.0041	0.0033	0.0030	0.0026	0.0023
MSE	4.21E-4	1.83E-4	1.64E-4	8.61E-5	3.86E-3

Table 3 indicates the estimated parameters for the simulated data by various temperatures based on the ISBO algorithm. According to the results, the proposed ISBO algorithm gives small enough results for MSE values for all temperatures. Besides, it is observed that the estimated data achieved by the improved SBO algorithm has proper confirmation with the simulated data for various temperatures.

By a glance on the results reported by Table 3 and Table 4, it can be concluded that by increasing the value of the parameter (except I_L and B) the temperature has been gradually increased.

The estimated parameters for the simulated data by different pressures based on the ISBO algorithm are given in Table 4. As can be seen, while different from the results at different temperatures, the values of the estimated parameters are close at different pressures, the parameter E0 has been increased by increasing the pressure.

Table 4. The estimated parameters for the simulated data by various pressures based on the ISBO algorithm

Variables	1 atm	3 atm	5 atm	7 atm	9 atm
$E_{oc}(V)$	1.076	1.113	1.126	1.132	1.145
$A(V)$	0.0250	0.0250	0.0250	0.0250	0.0250
$I_{o,a}(mA.cm^{-2})$	22.146	22.108	22.137	22.139	22.144
$I_{o,c}(mA.cm^{-2})$	4.452	4.436	4.439	4.438	4.438
$B(V)$	0.0742	0.741	0.0742	0.0742	0.0742
$I_L(mA.cm^{-2})$	160.053	160.053	160.056	160.053	160.058
$R_{ohm}(K\Omega.cm^{-2})$	0.0031	0.0031	0.0031	0.0031	0.0031
MSE	1.84E-4	1.86E-4	1.87E-4	1.89E-4	1.88E-4

Fig. (4) and Fig. (5) show the output voltage errors for the simulated data in Fig. (1) and Fig. (2).

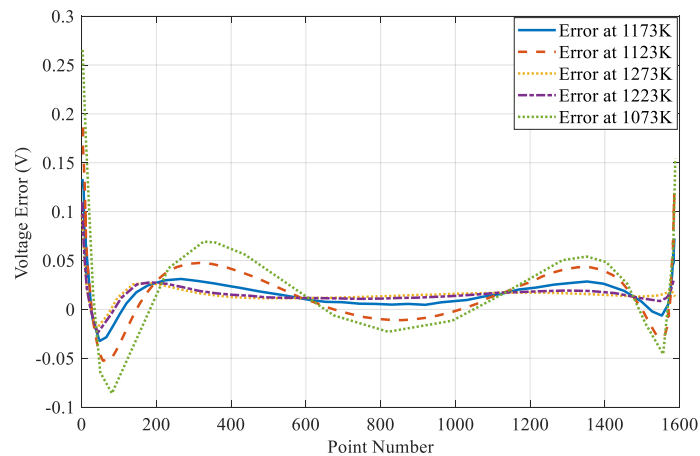


Figure 4. The voltage deviation between the simulated data and the data obtained by ISBO at different temperatures

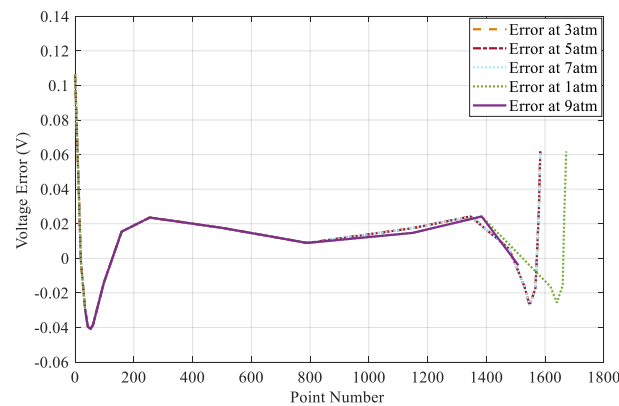


Figure 5. The voltage deviation between the simulated data and the data obtained by ISBO at different pressures

As observed in Figs. (4) and (5), there is a proper confirmation between the estimated data and the simulated data with a small MSE value.

5.2. Validation based on experimental data-ASC/SOFC

Besides, to validate the results based on simulated data, two different kinds of empirical data are used in this paper. The first data set is achieved by [33], which is based on a single cell $10 \times 10 \text{ cm}^2$ ASC-10B Elcogen planar (ASC-SOFC). This data contains 8 data sets with different fuel uses and temperatures. The estimated parameters based on the improved SBO algorithm have been reported in Table 5. In Table 7, case 1, 2, 4 mean dry H_2 at 599.85°C , 649.85°C , and 699.85°C , respectively; case 3 shows synthetic reformat at 649.85°C ; case 5 illustrates dry H_2 at FU 20%; case 6, 7, 8 demonstrate synthetic reformat at FU 20%, FU 50%, and FU 50% D humidified air, respectively.

Table 5. Identified parameters based on the ISBO algorithm for the empirical data of ASC-SOFC

Variables	Case 1	Case 2	Case 3	Case 4	Case 5	Case 6	Case 7	Case 8
$E_{oc}(V)$	1.185	1.620	1.367	1.004	1.632	1.007	1.003	1.007
$A(V)$	0.063	0.069	0.034	0.015	0.037	0.027	0.031	0.116
$I_{o,a}(mA.cm^{-2})$	2.415	7.641	2.463	31.24	1.935	20.28	30.42	30.45
$I_{o,c}(mA.cm^{-2})$	2.241	7.497	1.959	30.16	1.781	18.76	30.16	30.16
$B(V)$	0.003	2.16E-15	0.549	6.86E-15	7.86E-15	0.187	0.326	0.111
$I_L(mA.cm^{-2})$	168.48	171.48	202.14	196.67	174.21	121.52	199.24	200.00
$R_{ohm}(K\Omega.cm^{-2})$	4.97E-15	1.14E-16	1.72E-3	1.68E-3	1.11E-3	6.16E-3	6.19E-4	2.08E-10
MSE	5.06E-6	2.35E-6	2.76E-6	2.93E-6	1.17E-6	5.47E-7	1.48E-7	1.42E-6

Fig. (6) and Fig. (7) show the comparisons between the empirical ASC-SOFC data and the optimized model based on the IBSO algorithm during different temperatures and fuel utilization, respectively.

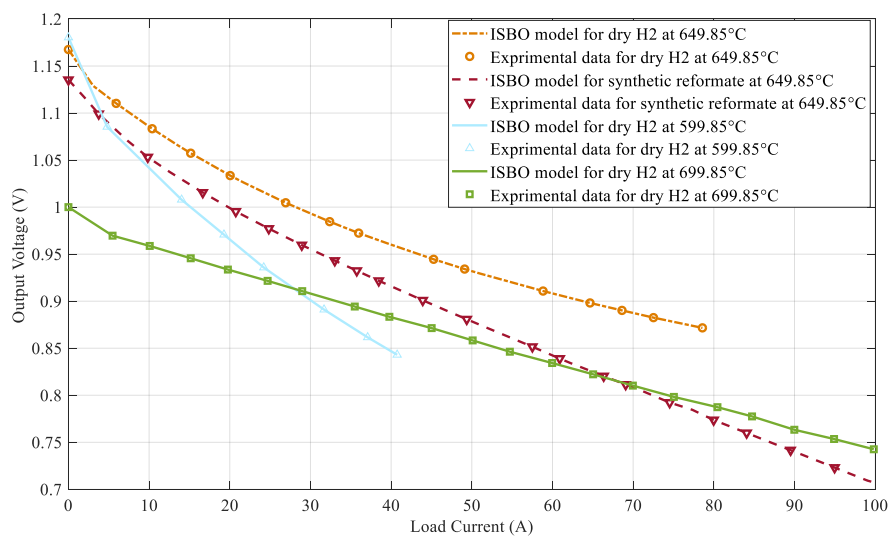


Figure 6. The comparisons between the empirical ASC-SOFC data and the optimized model based on IBSO algorithm during different temperatures

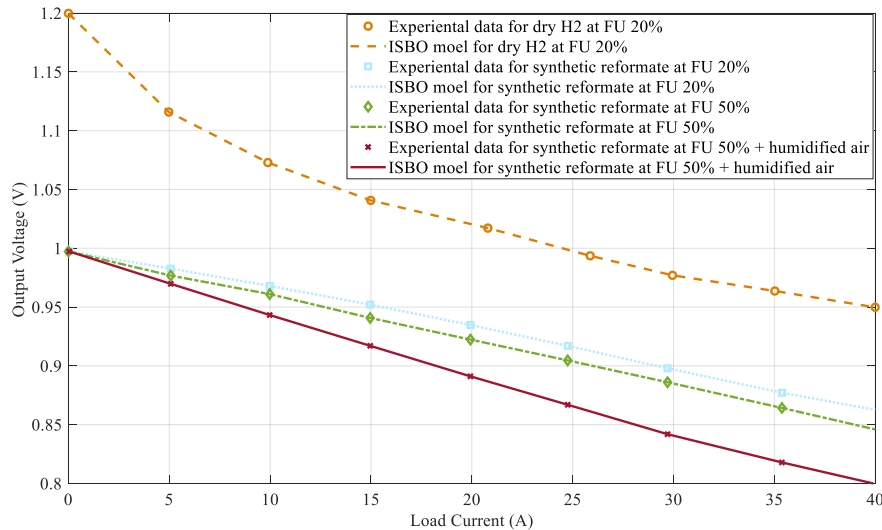


Figure 7. The comparisons between the empirical ASC-SOFC data and the optimized model based on ISBO algorithm during different fuel utilizations

As can be observed from Fig. (6) and Fig. (7), the estimated data based on the ISBO method have proper confirmation with the empirical data.

5.3. Validation based on comparison with other metaheuristics

In the previous subsections, the proposed ISBO-based method efficiency was verified on simulated data and also experimental data of a SOFC. In this part, the performance of the proposed ISBO algorithm is validated for showing its prominence toward the basic Satin Bowerbird Optimization algorithm (SBO) [34] and some other metaheuristics in the literature including Differential evolution algorithms (DE)[16], coRNA-GA [35], Chaotic Binary Shark Smell Optimization [17], swarm optimizer for parameter [36] for optimal parameter estimation of SOFC model. To do a fair comparison among different algorithms, similar numbers of population have been adopted for the algorithms (N=100) and the maximum iteration (Ni=30) is considered as the stopping criteria. Due to the random process of metaheuristics, 50 independent runs have been simulated for each algorithm to have a meaningful result in terms of statistical calculations. The results of the analyzed metaheuristics are indicated in Table 6.

Table 6. The comparison results of the MSE for various metaheuristics for the simulated data at various temperatures

Algorithms	549.85°C	649.85°C	699.85°C	749.85°C	799.85°C
SO [36]	1.23E-2 (4.15E-3)	2.84E-2 (4.09E-3)	1.62E-2 (4.32E-3)	8.77E-2 (2.63E-1)	1.25 (5.26E-1)
BSSO [17]	3.31E-2 (2.12E-2)	4.17E-2 (1.69E-2)	1.78E-2 (4.28E-2)	6.81E-1 (3.91E-1)	1.47 (8.98E-1)

coRNA-GA [35]	1.98E-2 (1.57E-2)	1.97E-2 (2.71E-2)	5.32E-2 (5.79E-2)	1.58E-1 (4.37E-1)	3.54 (7.59E-1)
DE [16]	4.59E-3 (9.97E-3)	9.52E-3 (8.96E-3)	2.28E-2 (6.45E-2)	6.27E-2 (3.34E-1)	7.34E(-2) (8.78E-2)
SBO [34]	1.59E-2 (1.89E-2)	2.26E-2 (1.89E-2)	7.36E-2 (9.94E-2)	1.29E-1 (3.31E-1)	5.34E-1 (9.35E-1)
ISBO	6.32E-4 (6.78E-4)	1.18E-3 (1.92E-3)	3.94E-3 (4.38E-3)	2.95E-3 (6.41E-3)	1.73E-3 (2.22E-4)

To provide a proper comparison between the IBSO method and the compared methods, the paired Wilcoxon signed-rank test [49] has been utilized. Fig. (8) shows the convergence speeds of the analyzed algorithms using the results achieved by Table 7. As can be seen, the proposed ISBO gives less average MSE and standard deviation values toward the basic SBO method and other compared metaheuristics that indicates its more robustness and precision.

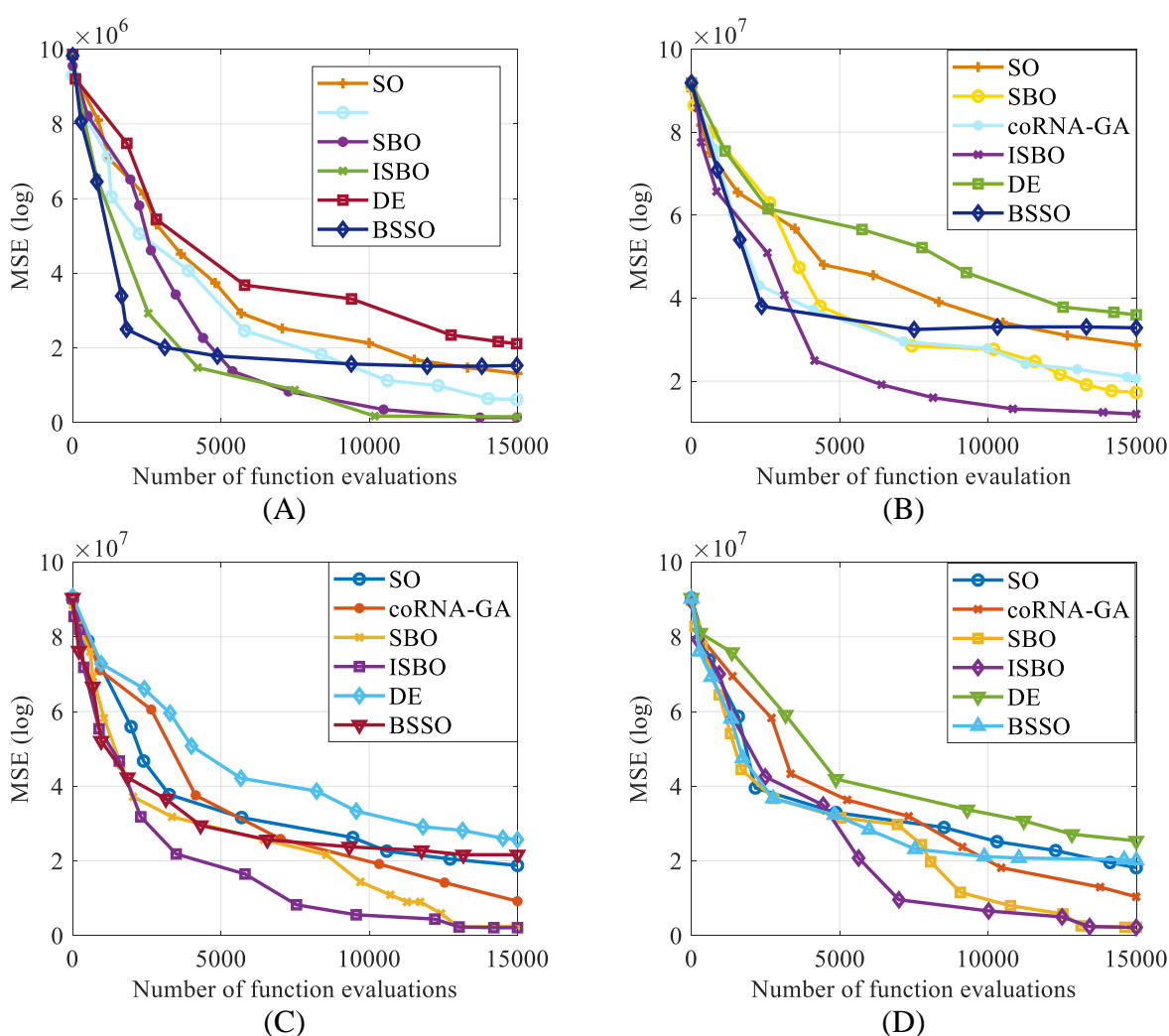


Figure 8. The convergence speeds of the analyzed algorithms for (A) 799.85, (B) 999.85, (C) 3 atm, and (D) 7 atm

Based on the Wilcoxon's test results, the ISBO method meaningfully has better efficiency than the other compared methods for different temperatures. Fig. (8) also shows that ISBO has the best convergence speed toward the others. However, the BSSO algorithm results in good convergence in the first stages, it failed to complete its good convergence until the end.

6. CONCLUSIONS

The present study proposed a new improved version of a new metaheuristic, called Improved Satin Bowerbird Optimization (ISBO) algorithm for optimal selection of unknown parameters of the SOFC model. The idea was to present a precise model with optimal parameters such that it gives a good agreement of the voltage vs. current profile of the SOFC. To evaluate the model accuracy, the mean squared error (MSE) was employed as a cost function between the achieved data and the empirical data. For evaluating the capability of the proposed ISBO method, it was simulated based on three different scenarios. In the first scenario, the method was evaluated by modeling simulated data. In the next scenario, the method was used to model an experimental system (ASC-SOFC). Finally, the method was compared with basic Satin Bowerbird Optimization algorithm (SBO), and some other metaheuristics in the literature including Differential evolution algorithms (DE), coRNA-GA, Chaotic Binary Shark Smell Optimization, and Swarm Optimizer (SO) for the parameter for optimal parameter estimation of SOFC model. The method was finally compared with these algorithms from the points of convergence speed and accuracy to show its robustness and precision toward the others.

ACKNOWLEDGEMENT

This research work is based on the support of "2019 Woosong University Academic Research Funding."

References

1. H. Khodaei, M. Hajiali, A. Darvishan, M. Sepehr and N. Ghadimi, *Appl. Therm. Eng.*, 137 (2018) 395.
2. G. Aghajani, N. Ghadimi, *Energy Rep.*, 4 (2018) 218.
3. Z. Yin, N. Razmjooy, *Int. J. Power Energy Syst.*, 40 (2020).
4. A. R. Gollou, N. Ghadimi, *J. Intell. Fuzzy Syst.*, 32 (2017) 4031.
5. F. Mirzapour, M. Lakzaei, G. Varamini, M. Teimourian and N. Ghadimi, *J. Ambient Intell. Hum. Comput.*, 10 (2019) 77.
6. M. Hosseini Firouz, N. Ghadimi, *Complexity*, 21 (2016) 70.
7. Z. Yuan, W. Wang, H. Wang and N. Razmjooy, *Energy Rep.*, 6 (2020) 662.
8. M. Hamian, A. Darvishan, M. Hosseinzadeh, M.J. Lariche, N. Ghadimi and A. Nouri, *Eng. Appl. Artif. Intell.*, 72 (2018) 203.
9. C. Wang, M.H. Nehrir, *IEEE Trans. Energy Convers.*, 22 (2007) 887.
10. H. A. Bagal, Y.N. Soltanabad, M. Dadjuo, K. Wakil and N. Ghadimi, *Sol. Energy*, 169 (2018) 343.
11. D. Yu, N. Ghadimi, *IET Renewable Power Gener.*, 13 (2019) 2587.
12. X. Fei, R. Xuejun and N. Razmjooy, *Energy Sources Part A*, (2019) 1.
13. M. W. Tian, S.R. Yan, S.Z. Han, S. Nojavan, K. Jermsittiparsert and N. Razmjooy, *J. Cleaner*

- Prod.*, 249 (2020) 119414.
14. M. H. Firouz, N. Ghadimi, *J. Intell. Fuzzy Syst.*, 30 (2016) 845.
 15. J. Yang, X. Li, J. H. Jiang, L. Jian, L. Zhao, J.G. Jiang, X.G. Wu and L.H. Xu, *Int. J. Hydrogen Energy*, 36 (2011) 6160.
 16. Y. Liu, W. Wang and N. Ghadimi, *Energy*, 139 (2017) 18.
 17. Y. Wei, R. J. Stanford, *Energy*, 88 (2019) 115770.
 18. L. Jun, C. Chen, Zh. Liu, K. Jermsittiparsert and N. Ghadimi, *J. Storage Mater*, 27 (2020) 101057.
 19. G.A. Bunin, Z. Wuillemin, G. François, A. Nakajo, L. Tsikonis and D. Bonvin, *Energy*, 39 (2012) 54.
 20. A. Gebregergis, P. Pillay, D. Bhattacharyya and R. Rengaswemy, *IEEE Trans. Ind. Electron*, 56 (2008) 139.
 21. S. Chan, C. Low and O. Ding, *J. Power Sources*, 103 (2002) 188.
 22. M. Qing, T. Liu, C. Su, H. Niu, Zh. Hou and N. Ghadimi, *Int. J. Control Autom. Syst.*, 31 (2020) 257.
 23. S. Chan, K. Khor and Z. Xia, *J. Power Sources*, 93 (2001) 130.
 24. M. Gheydi, A. Nouri and N. Ghadimi, *IEEE Syst. J.*, 12 (2016) 2782.
 25. M. Saeedi, M. Moradi, M. Hosseini, A. Emamifar and N. Ghadimi, *Appl. Therm. Eng.*, 148 (2019) 1081.
 26. Y. Bengio, P. Lamblin, D. Popovici and H. Larochelle, *Adv. in neural inform. proc. Syst.*, (2007) 153.
 27. S.H.S. Moosavi, V.K. Bardsiri, *Eng. Appl. Artif. Intell.*, 60 (2017) 1.
 28. H. Ye, G. Jin, W. Fei and N. Ghadimi, *Energy Sources Part A*, (2020) 1.
 29. E. Çelik., *Eng. Appl. Artif. Intell.*, 87 (2020) 103294.
 30. H. Leng, X. Li, J. Zhu, H. Tang, Zh. Zhang and N. Ghadimi, *Adv. Eng. Inf.*, 36 (2018) 20.
 31. D. Yang, G. Li and G. Cheng, *Chaos, Solitons & Fractals*, 34 (2007) 1366.
 32. C. Rim, S. Piao, G. Li and U. Pak, *Soft Comput.*, 22 (2018) 621.
 33. C. Wei, R. Mohammaditab, G. Fathi, K. Wakil, A.G. Ebadi and N. Ghadimi, *Renewable Energy*, 143 (2019) 1.
 34. S. H. Samareh Moosavi, V. Khatibi Bardsiri, *Eng. Appl. Artif. Intell.*, 60 (2017) 1.
 35. N. Wang, D. Wang, Y. Xing, L. Shao and S. Afzal, *Renewable Energy*, (2020).
 36. G. Xiong, J. Zhang, D. Shi and X. Yuan, *Energy Convers. Manage.*, 203 (2020) 112204